



# Effect of abdominal adipose content on spine phantom bone mineral density measured by rapid kilovoltage-switching dual-energy CT and quantitative CT

Hang Ye<sup>1,2^</sup>, Xiaoyang Li<sup>1,2^</sup>, Ning Yao<sup>1,2</sup>, Yuting Shi<sup>1,3</sup>, Yujiao Wang<sup>1,2</sup>, Wanjiang Yu<sup>1,2,3^</sup>

<sup>1</sup>Department of Radiology, Qingdao Municipal Hospital, The Third Affiliated Medical College of Qingdao University, Qingdao, China;

<sup>2</sup>Department of Imaging Medicine and Nuclear Medicine, Dalian Medical University, Dalian, China; <sup>3</sup>Department of Imaging Medicine and Nuclear Medicine, Weifang Medical College, Weifang, China

**Contributions:** (I) Conception and design: W Yu, H Ye; (II) Administrative support: W Yu; (III) Provision of study materials or patients: X Li; (IV) Collection and assembly of data: X Li, N Yao, Y Shi; (V) Data analysis and interpretation: H Ye, Y Wang; (VI) Manuscript writing: All authors; (VII) Final approval of manuscript: All authors.

**Correspondence to:** Wanjiang Yu. Department of Radiology, Qingdao Municipal Hospital, The Third Affiliated Medical College of Qingdao University, 51 Donghai West Road, Shinan District, Qingdao 266071, China. Email: yuwj169@sina.com.

**Background:** The purpose of this study was to investigate the effect of abdominal adiposity, as measured by abdominal total adipose tissue (TAT), on the accuracy of rapid kilovoltage-switching dual-energy computed tomography (DECT) and quantitative computed tomography (QCT) measurements of bone mineral density (BMD) in a spine phantom model.

**Methods:** Fresh porcine fat was wrapped around the European Spine Phantom (ESP) and divided into four groups according to the TAT cross-sectional areas,  $S=0, 100, 200, \text{ and } 350 \text{ cm}^2$ , to simulate different TAT contents. The hydroxyapatite (HAP) (water) values of each vertebra were measured by DECT, and the BMD values by QCT. A one-sample *t*-test was used to analyze the differences between the measurements and the true values of the ESP. One-way analysis of variance (ANOVA) was applied to compare the differences between measurements under different TAT conditions, and the root-mean-square errors (RMSEs) of the BMD measurements were calculated and compared. Moreover, Pearson's correlation analysis was performed for the RMSE and TAT. Linear regression analysis was conducted on the measurements, the true values, and the TAT to obtain the correction equations for the BMD and to compare the RMSE before and after correction.

**Results:** At higher TAT content, the measurements of both scanning methods were more affected, and the measurements of the  $TAT = 350 \text{ cm}^2$  group were significantly different from the remaining groups ( $P < 0.05$ ). There was a positive correlation between the RMSE and TAT ( $r > 0, P < 0.05$ ), with the RMSE of the L1 vertebrae the largest under the same TAT content. The corrected equations for BMD were derived, and the RMSE of BMD was significantly reduced after correction.

**Conclusions:** The measurements of ESP BMD for both rapid kilovoltage-switching DECT and QCT changed with TAT content. Along with the increase of TAT, the RMSE of measurements increased and the accuracy decreased; moreover, the lower the value of BMD, the more significant the RMSE. The linear regression analysis allowed the corrected BMD measurements to be very close to true values.

**Keywords:** Quantitative CT (QCT); dual-energy CT (DECT); abdominal adipose; bone mineral density (BMD)

<sup>^</sup> ORCID: Hang Ye, 0000-0003-2023-3015; Xiaoyang Li, 0000-0002-2080-1214; Wanjiang Yu, 0000-0002-0639-2258.

Submitted Jan 23, 2022. Accepted for publication Jul 08, 2022.

doi: 10.21037/qims-22-72

View this article at: <https://dx.doi.org/10.21037/qims-22-72>

## Introduction

Osteoporosis is one of the most common chronic metabolic bone diseases (1) and is associated with reduced bone mineral density (BMD), which increases the risk of fracture. The BMD is considered an important indicator for monitoring osteoporosis and estimating fracture risk, especially for women and the elderly (2,3). Therefore, accurate measurement of BMD is very important. With the development and clinical validation of quantitative computed tomography (QCT) technology, QCT has been widely employed for clinical BMD measurements (4-7). However, some studies have shown that abdominal and spinal bone marrow adipose content influences the QCT measurements of vertebral BMD (8-13). Dual-energy computed tomography (DECT) employs a high- and low-energy switching scanning method with a material decomposition (MD) technique that also allows the accurate measurement of vertebral BMD, which has shown preliminary advantages (14-17). However, it is possible that the DECT measurements of BMD were influenced, to some extent, by abdominal adipose content. Metabolic syndrome, type 2 diabetes, and, in particular, overweight and obesity have been recognized as an epidemic (18,19). Moreover, abdominal adipose content varies considerably between individuals, and the influence of abdominal adipose content on the measurement of BMD is not yet clearly established. It is well known that abdominal adipose content is much greater than that of bone marrow; the adipose content of bone marrow is comparatively negligible to abdominal adipose content. Therefore, this study simulated different levels of abdominal total adipose tissue (TAT) and investigated their effect on the bone density of the European Spine Phantom (ESP) measured by rapid-kilovoltage-switching DECT and QCT. We present the following article in accordance with the MDAR reporting checklist (available at <https://qims.amegroups.com/article/view/10.21037/qims-22-72/rc>).

## Methods

### Phantom

The ESP (QRM GmbH, Moehrendorf, Germany) (20) used in this study was composed of epoxy resin and three

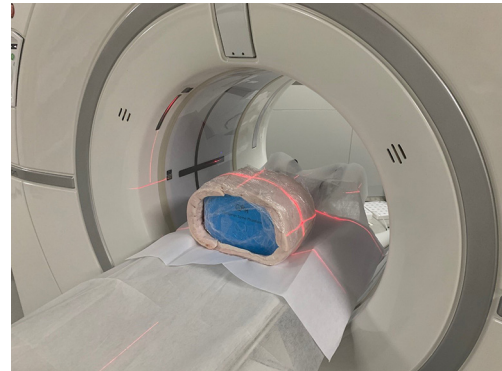


**Figure 1** Revolution CT scanner scans the phantom wrapping porcine-isolated fat. CT, computed tomography.

hydroxyapatite (HAP) inserts of densities 50 mg/cm<sup>3</sup> (osteoporotic), 102 mg/cm<sup>3</sup> (osteopenia), and 197 mg/cm<sup>3</sup> (normal), labeled as the first lumbar vertebra (L1), second lumbar vertebra (L2), and third lumbar vertebra (L3), respectively. Three pieces of fresh (within 6 h after slaughter) porcine-isolated fat (without skin) of different sizes were selected and wrapped around the ESP (*Figure 1*) to simulate different levels of human abdominal TAT.

### TAT area measurement

Three pieces of porcine-isolated fat were wrapped around the ESP separately, and scanned by QCT protocol using a 256-section rapid kilovoltage-switching DECT scanner (Revolution CT, GE Healthcare, Waukesha, WI, USA). The scanning parameters were as follows: tube voltage of 120 kV, tube current of 200–370 mA using automatic milliamperage technology, tube speed of 0.8 s/r, and a pitch of 0.992:1. The reconstructed 1.25 mm thin-layer CT images were transferred to the QCT workstation (Mindways Software Inc., Austin, TX, USA), and the TAT area at the L2 central level was measured using the “Tissue Composition Analysis” function (*Figure 2*), resulting in three porcine-isolated fat areas of approximately 100, 200, and 350 cm<sup>2</sup>, respectively, with TAT = 350 cm<sup>2</sup> representing the average abdominal TAT of the clinically overweight/obese population. In this study, four groups were divided according to different TAT areas (S): S=0, 100, 200, and 350 cm<sup>2</sup>. Given that quality control

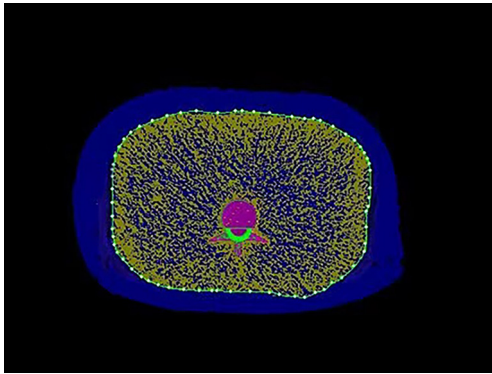


**Figure 2** Quantitative CT measurement of the total adipose tissue area at the second lumbar vertebral center level of the phantom. Quantitative CT coloring of the different components, the green aperture close to the outer edge of the phantom, the mixed blue and yellow part inside the green aperture is the water-equivalent material, the pink part is the vertebrae, and the blue part outside the green aperture is the measured area, which is the total adipose tissue area of the anthropomorphic. CT, computed tomography.

procedures must be performed prior to using the software, the quality assurance phantom was scanned using 120 kV tube voltage and automatic mA parameters, and then the images were transferred to the QCT Mindways workstation for quality control with the “New Quality Assurance Exam Analysis” function.

### **BMD data acquisition and image reconstruction**

The GE Revolution CT scanner was used to perform DECT scanning and QCT scanning on each of the four groups of ESP. The DECT imaging parameters were as follows: tube voltage for fast switching of 80–140 kV, tube current of 230 mA, tube speed of 0.8 s/r, and a pitch of 0.992:1. A total of 10 scans were conducted per group, with repositioning after each scan to assess the stability of the measurements and calculate the average value for each group. The reconstructed 1.25 mm thin-layer CT images after DECT scanning were transferred to an advanced workstation (ADW4.6; GE Medical Systems, Milwaukee, WI, USA), using the “MD Analysis” function in Gemstone Spectral Imaging (GSI) viewer software (GE Healthcare, USA). The principle for this approach is that the X-ray attenuation of each substance can be represented by two “base substances”, of which water and iodine are the two most commonly used base materials,

and the bone mineral is represented by HAP; therefore, the quantitative determination of HAP becomes the key to the diagnosis of osteoporosis. Mu *et al.* (21) studied human patients and indicated that a DECT scan with HAP-water as the base material pair has good accuracy and high application value in the clinical diagnosis of osteoporosis. Therefore, MD images were obtained with HAP-water as the base material pair in this study, and the HAP (water) values were measured for L1, L2, and L3 vertebrae.

The imaging parameters for QCT were set as follows: tube voltage of 120 kV, tube current of 200–370 mA using automatic milliamp technique, tube speed of 0.8 s/r, and a pitch of 0.992:1. A total of 10 scans were conducted per group, with repositioning in between scans. In addition, the same level of quality control was required before using the QCT measurement software. Then, the reconstructed 1.25 mm thin-layer CT images from the QCT scan were transferred to the QCT Mindways workstation to measure the BMD values of the L1, L2, and L3 vertebrae. For the above two kinds of image post-processing, a region of interest with a size of 15 mm × 15 mm was placed in the center of each vertebral body (*Figure 3*).

### **Statistical analysis**

The software package SPSS 25.0 (IBM Corp., Armonk, NY, USA) was used for data analysis, and since the true values of phantom BMD were known in this study, a one-sample *t*-test was used to compare the differences between the measurements and the true values of BMD for both scanning methods. Using GraphPad Prism 9.2.0 (GraphPad Software, San Diego, CA, USA) software, the one-way analysis of variance (ANOVA) test followed by the post hoc Tukey honest significant difference (HSD) test was employed to compare the differences between measurements at different TAT conditions for each vertebra of DECT and QCT, respectively. Differences were considered statistically significant at  $P < 0.05$ . The software MATLAB 9.9.0 (MathWorks, Natick, MA, USA) was used to calculate and compare the root-mean-square error (RMSE) of the DECT and QCT BMD measurements. The RMSE is the square root of the ratio of the deviation between the measured value and the true value and the number of measurements ( $N$ ). In this study,  $N=10$ ; the RMSE can reflect the accuracy of the measurement very well, with the formula:

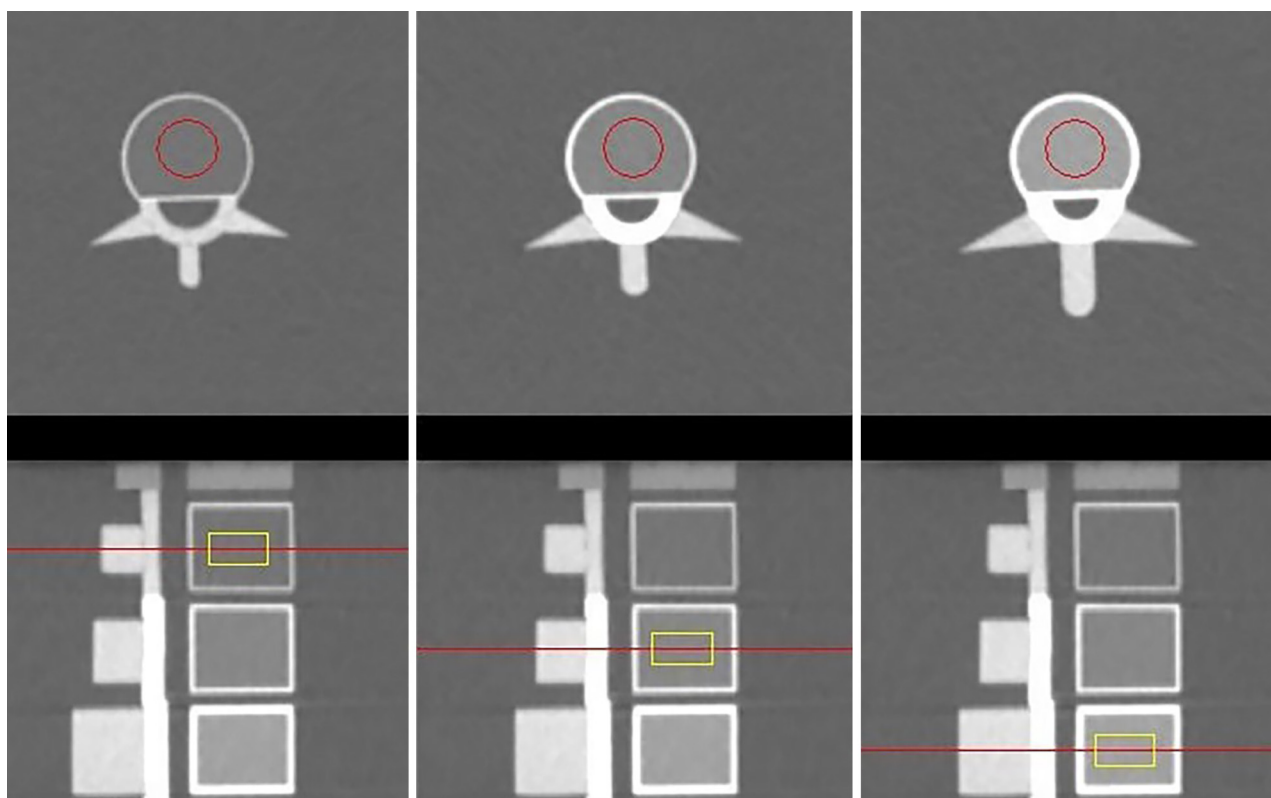


**Figure 3** Quantitative CT measurements of the first, second, and third lumbar vertebrae BMD. Red circles represent the axial region of interest, and yellow squares represent the sagittal region of interest. CT, computed tomography; BMD, bone mineral density.

$$RMSE = \sqrt{\frac{\sum_{i=1}^N (y_i - \hat{y}_i)^2}{N}} \quad [1]$$

Linear correlation analysis was performed to assess the relationship between the RMSE and TAT based on Pearson's correlation coefficient, and a significant correlation between the parties of difference was considered at  $P < 0.05$ . Linear regression analysis was conducted to derive calibration equations for the measurements of the two scanning methods and to compare the RMSE of the measurements before and after calibration.

## Results

### *Comparison of DECT and QCT BMD measurements with true phantom values*

Comparison of HAP (water) measurements of L1, L2, and L3 vertebrae on DECT using true values (*Table 1*) showed that there were statistically significant differences between HAP (water) measurements and true values in all groups

( $P < 0.05$ ), except in the lower TAT groups (TAT = 0, 100, and 200  $\text{cm}^2$ ) for the L2 vertebrae where there were no statistically significant differences ( $P > 0.05$ ). A comparison of the L1, L2, and L3 vertebral BMD measurements of QCT with the true values (*Table 2*) showed that the measurements were significantly different from the true values in all groups ( $P < 0.001$ ). It can be observed from *Tables 1, 2* that different contents of TAT have different degrees of influence on the accuracy of BMD measurement by both DECT and QCT.

### *Comparison between BMD measurements for different TAT conditions*

The comparison of the measurements at different TAT conditions for DECT and QCT (*Figure 4*) shows that the differences between the measurements in the lower TAT groups (TAT = 0, 100, and 200  $\text{cm}^2$ ) were not statistically significant ( $P > 0.05$ ), although the measurements in the TAT = 350  $\text{cm}^2$  group were significantly different from the rest of the groups ( $P < 0.05$ ). Among them, there was no statistically

**Table 1** Comparison of HAP (water) measurements with true values for each vertebral body on DECT

TAT (cm <sup>2</sup> )	L1 (50 mg/cm <sup>3</sup> )		L2 (102 mg/cm <sup>3</sup> )		L3 (197 mg/cm <sup>3</sup> )	
	HAP (water) measurements	P value	HAP (water) measurements	P value	HAP (water) measurements	P value
0	51.23±2.48	0.03	101.34±1.12	0.10	194.89±1.28	0.001
100	53.55±2.60	0.002	101.58±2.15	0.55	193.04±2.08	<0.001
200	54.33±1.85	<0.001	103.93±2.80	0.06	193.37±3.97	0.02
350	60.46±3.97	<0.001	111.86±3.62	<0.001	192.56±4.65	0.01

Data are expressed as mean ± SD. L1, L2 and L3 represent vertebrae of different bone mineral density. HAP (water), hydroxyapatite-water as the base material pair; DECT, dual-energy computed tomography; TAT, total adipose tissue; SD, standard deviation.

**Table 2** Comparison of BMD measurements with true values for each vertebral body on QCT

TAT (cm <sup>2</sup> )	L1 (50 mg/cm <sup>3</sup> )		L2 (102 mg/cm <sup>3</sup> )		L3 (197 mg/cm <sup>3</sup> )	
	BMD measurements	P value	BMD measurements	P value	BMD measurements	P value
0	41.09±1.33	<0.001	98.70±0.96	<0.001	192.97±1.86	<0.001
100	38.86±1.07	<0.001	96.92±0.96	<0.001	191.94±1.88	<0.001
200	35.97±1.08	<0.001	94.91±0.97	<0.001	189.29±1.91	<0.001
350	32.55±2.09	<0.001	91.11±1.77	<0.001	183.90±1.73	<0.001

Data are expressed as mean ± SD. L1, L2 and L3 represent vertebrae of different bone mineral density. BMD, bone mineral density; QCT, quantitative computed tomography; TAT, total adipose tissue; SD, standard deviation.

significant difference ( $P>0.05$ ) between the measurements of each group (TAT =0, 100, 200, and 350 cm<sup>2</sup>) when the L3 vertebral body was scanned by DECT. Overall, these results indicate that the higher the TAT, the greater its effect on DECT and QCT measurements.

### RMSE of the BMD measurements of DECT and QCT

The RMSE of the DECT measurements were all smaller than the QCT (Table 3). There was a strong positive correlation between RMSE and TAT for each vertebral measurement in both scanning methods ( $r>0$ ;  $P<0.05$ ) (Figure 5), indicating that the RMSE increased with increasing TAT. Furthermore, for TAT >100 cm<sup>2</sup>, the RMSE of L1 vertebrae was always greater than that of L2 and L3 vertebrae.

### Linear regression analysis

In order to obtain BMD measurements of DECT and QCT closer to the true value of the phantom and to reduce the RMSE, a linear regression analysis of DECT and QCT measurements, using true values of the phantom

and TAT, was performed. The correction equations of the measurements were obtained as:

DECT: ( $R^2=0.996$ )

$$Y(BMD) = 1.058 \times \text{measurement} - 0.018 \times TAT - 5.248 \quad [2]$$

QCT: ( $R^2=0.998$ )

$$Y(BMD) = 0.968 \times \text{measurement} + 0.024 \times TAT + 8.57 \quad [3]$$

To verify the applicability and validity of the correction equation, an additional group with TAT of 320 cm<sup>2</sup> (i.e., a separate data set), was added to this study, and the experimental methods applied were identical to those of all the above groups. The BMD measurements and the RMSE of DECT and QCT were obtained, and the RMSE of the measurements were significantly reduced by the correction equation (Table 4, Figure 6).

## Discussion

### Current status of application of BMD measurement by DECT and QCT

Currently, QCT and dual-energy X-ray absorptiometry (DXA) are the commonly used methods for measuring BMD. The DXA measurements focus on areal bone mineral

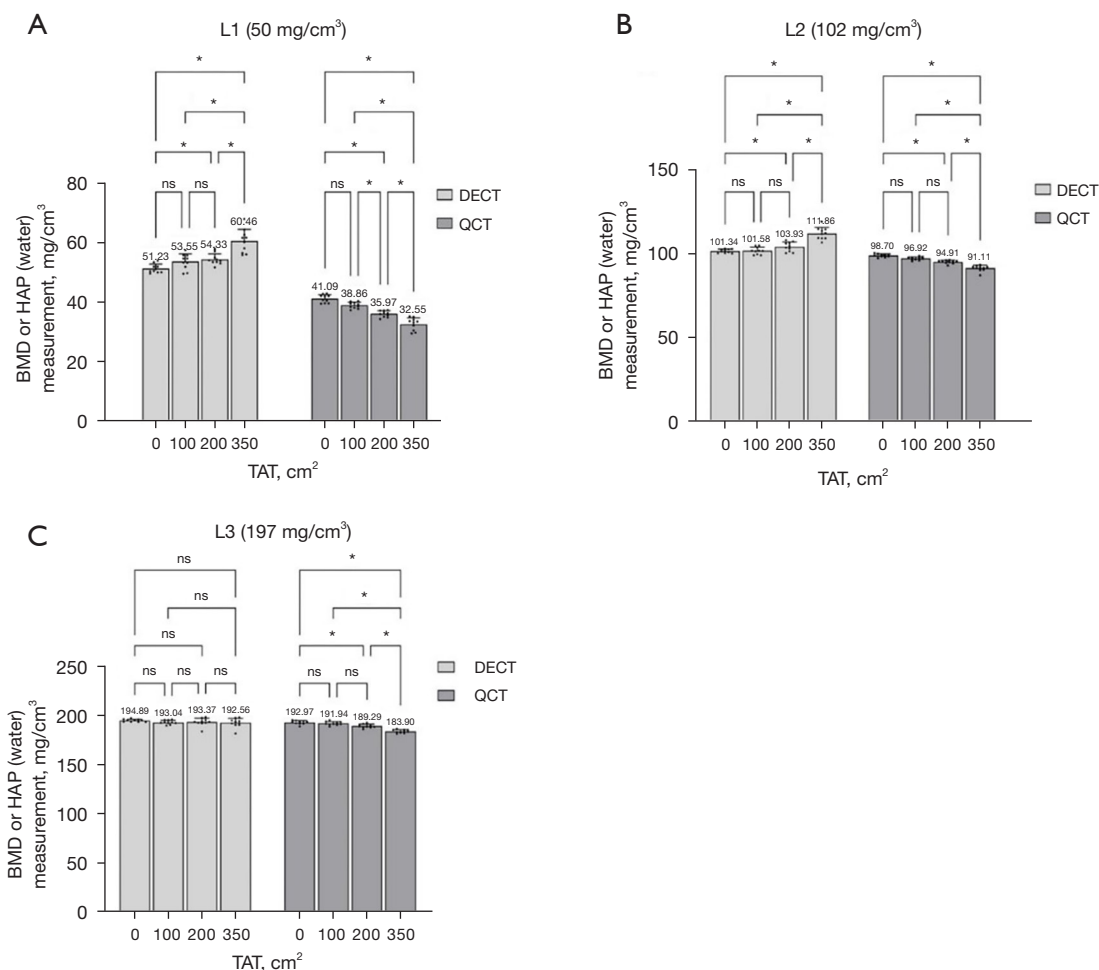


**Figure 4** DECT scan (light gray bars) and QCT scan (dark gray bars), comparison between measurements with different TAT conditions. L1 (A), L2 (B), and L3 (C) represent vertebrae of different BMD. ns, P>0.05, \*, P<0.05 (ns, no significant). The differences between the measurements of the TAT =350 cm<sup>2</sup> group and the rest of the groups were the most significant. BMD, bone mineral density; HAP, hydroxyapatite; DECT, dual-energy computed tomography; QCT, quantitative computed tomography; TAT, total adipose tissue.

**Table 3** RMSE of the BMD measurements of DECT and QCT

TAT (cm <sup>2</sup> )	L1 (50 mg/cm <sup>3</sup> )		L2 (102 mg/cm <sup>3</sup> )		L3 (197 mg/cm <sup>3</sup> )	
	DECT	QCT	DECT	QCT	DECT	QCT
0	0.42	2.01	0.28	0.76	0.54	0.98
100	0.97	2.50	0.47	1.15	0.99	1.20
200	1.05	3.15	0.93	1.60	1.17	1.77
350	2.49	3.93	2.33	2.46	1.40	2.95

L1, L2 and L3 represent vertebrae of different bone mineral density. RMSE, root-mean-square error; BMD, bone mineral density; DECT, dual-energy computed tomography; QCT, quantitative computed tomography; TAT, total adipose tissue.

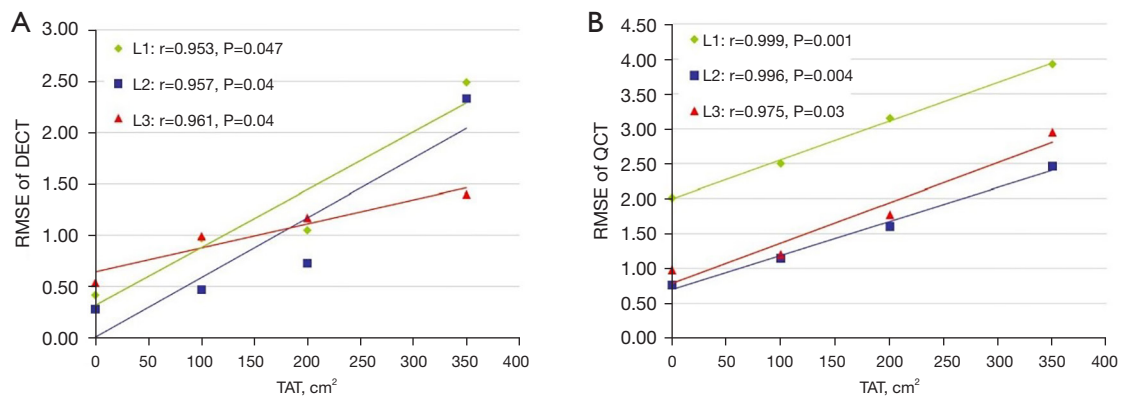


**Figure 5** The RMSE of the measurements for each vertebra (L1 green line, L2 blue line, L3 red line) of the DECT (A) and QCT (B) showed a strong positive correlation with TAT, which means that the RMSE of the measurements increased with increasing TAT, and the RMSE of L1 was almost always the largest under the same TAT condition. RMSE, root-mean-square error; DECT, dual-energy computed tomography; TAT, total adipose tissue; QCT, quantitative computed tomography.

**Table 4** BMD measurements of DECT and QCT at TAT =320 cm<sup>2</sup> and RMSE before and after correction by linear regression analysis

Variables	L1 (50 mg/cm <sup>3</sup> )		L2 (102 mg/cm <sup>3</sup> )		L3 (197 mg/cm <sup>3</sup> )	
	DECT	QCT	DECT	QCT	DECT	QCT
BMD	57.99±2.09	35.23±2.46	110.78±3.25	91.85±1.21	195.07±3.42	184.83±3.22
RMSE	1.84	3.34	2.08	2.29	0.85	2.81
RMSE-corrected	0.47	0.51	1.17	0.75	0.85	0.78

BMD data are expressed as mean ± SD. L1, L2 and L3 represent vertebrae of different bone mineral density. BMD, bone mineral density; DECT, dual-energy computed tomography; QCT, quantitative computed tomography; TAT, total adipose tissue; RMSE, root-mean-square error; SD, standard deviation.

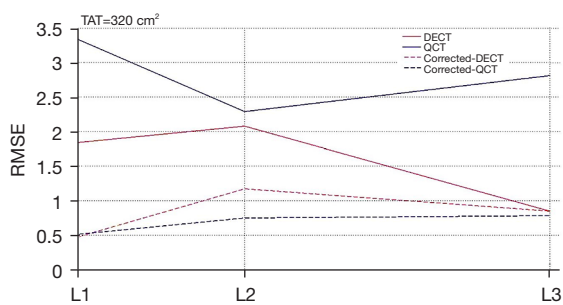


**Figure 6** The RMSE of the QCT (blue solid line) measurement is always higher than that of the DECT (red solid line). The RMSE of the BMD values for the corrected DECT (red dashed line) and the corrected QCT (blue dashed line) are significantly lower than those before correction. L1, L2 and L3 represent vertebrae of different bone mineral density. TAT, total adipose tissue; RMSE, root-mean-square error; DECT, dual-energy computed tomography; QCT, quantitative computed tomography; BMD, bone mineral density.

density (aBMD; g/cm<sup>2</sup>), whereas the QCT measurements focus on volumetric bone mineral density (vBMD; mg/cm<sup>3</sup>), thus avoiding inaccurate measurements due to projection overlap (22). In China, CT examinations have become an important routine screening method due to their low cost, and QCT may be potentially used for the opportunistic detection of osteoporosis in patients undergoing CT for other indications. In recent years, the clinical application of the rapid kilovoltage-switching DECT has gradually become more widespread. A DECT can reconstruct MD images based on the principles of MD and quantitative analysis and provide more accurate density measurements for various base materials (such as HAP). Cui *et al.* (23) showed that the Revolution DECT, with a 0.8 s/r tube speed and a 230-mA tube current as imaging parameters, and the employment of HAP-water base material pair to measure BMD can further ensure the accuracy of the measurement. Li *et al.* (24) demonstrated that both QCT

and DECT can accurately measure BMD by scanning ESP. This study showed that the RMSE of both DECT and QCT measurements for each vertebra was the smallest when  $TAT = 0 \text{ cm}^2$ ; that is, when no adipose tissue was wrapped around the phantom. With the increase of TAT, the RMSE of both scanning modes also gradually increased.

#### *Effect of TAT on BMD measurements*

Most previous studies have not considered the effect of adipose tissue on the BMD measurements obtained by DECT and QCT. Although there is no definitive conclusion about its effect, our previous study (25) showed that abdominal adipose tissue had some influence on BMD measurement results. Javed *et al.* (26) used DXA to measure the BMD of a bovine femur and found that as the fat layer around the femur increased, the BMD also gradually increased. Although the scanning method and the object of measurement used in this study were different, the conclusion remains informative. Yu *et al.* (12) used DXA and QCT scans of ESP wrapped in different thicknesses of fat layers and found that increasing the thickness of the fat resulted in decreased QCT BMD measurements, forming measurement errors, but with less and more uniform measurement errors compared to DXA BMD measurements.

The results of this study showed that TAT influenced the accuracy of both DECT and QCT measurements of BMD. With increasing TAT, the BMD values of all vertebrae measured by QCT gradually decreased, which was consistent with the results of Yu *et al.* (12), and the HAP (water) values of L1 and L2 vertebrae measured by DECT gradually increased, yet there was no significant change in L3 vertebrae. In the comparison of measurements under different TAT conditions, there were significant differences between the  $TAT = 350 \text{ cm}^2$  group and the remaining groups ( $P < 0.05$ ), which also indicated that the higher the TAT, the greater the effect on measurements. In addition, the RMSE of both the DECT and QCT measurements in this study showed a strong positive correlation with TAT, further suggesting that the RMSE increased with the increasing TAT areas and the accuracy of the measurements decreased. Meanwhile, the RMSE of the L1 vertebrae was always greater than that for the L2 and L3 at the same TAT condition, which means that the lower the true value of vertebral BMD, the greater the RMSE of DECT and QCT measurements. In other words, the accuracy of measuring BMD was more affected by TAT. Therefore, clinically,

in patients with more severe osteoporosis, the effect of abdominal adipose content must be considered when measuring vertebral BMD with DECT and QCT.

#### *Measurement differences between DECT and QCT and correction methods for measurement errors*

Li *et al.* (24) showed that the measurement error of DECT was less than that of QCT in a phantom study. Our study showed that the RMSE of DECT was smaller than that of QCT, with L1 vertebrae being more significant, suggesting that when osteoporosis is present, the accuracy of BMD measured by DECT is higher than the BMD measured by QCT and is relatively less affected by TAT. The possible reason for this result is that the QCT is conducted by solving the equation to obtain the BMD value in comparison with the correction phantom. Moreover, under conventional scanning conditions (80–120 kV), the absorption attenuation curve of abdominal adipose for the X-ray shows a bow-back upward direction; that is, under the conditions of CT imaging, the absorption of X-rays by adipose increased with the increase of tube voltage (27). Therefore, the effect of TAT cannot be overcome when using QCT to measure BMD, and the higher the TAT content, the greater the measurement errors and the more measured values that are affected. In contrast, the DECT in this study used the HAP-water decomposition method, and the main components of ESP vertebrae were equivalent to HAP and water, so the DECT measurements were relatively less affected by TAT. Furthermore, this study used linear regression analysis to obtain the correction equations for the BMD measurements, and after additional independent data sets, BMD measurements from the  $TAT = 320 \text{ cm}^2$  group were substituted into the equation for validation. It was found that the corrected BMD values were very close to the true values of the phantom and the RMSE was significantly decreased.

There were several limitations to our study. Firstly, only a small sample size of phantom experiments was involved in this study, and the conclusions have not been validated in clinical practice. Moreover, the findings of this study have not been validated in different CT scanners or imaging software. Secondly, the actual human body may be accompanied by changes in a variety of components, which are not reflected in this study, such as the ribs, intestinal tubes, gases, and intestinal contrast agents. Whether these components affect the accuracy of BMD measurements warrants further investigation. In addition,

further refinement of the effect of different contents of adipose tissue on different BMD measurements is needed. The vertebral BMD is  $80 \text{ mg/cm}^3$  and the mean abdominal TAT in the clinically overweight/obese population is approximately  $350 \text{ cm}^2$ , with a rare number of obese patients having abdominal TAT up to  $600\text{--}700 \text{ cm}^2$ , so further studies should incorporate more refined subgroups with a TAT greater than  $350 \text{ cm}^2$ .

In conclusion, when employing rapid kilovoltage-switching DECT or QCT to assist in the clinical assessment of BMD values in the lumbar spine for overweight/obese patients, the results may be subject to some errors. The errors will be most pronounced in older patients with overweight/obesity combined with osteoporosis. Moreover, the measurement errors of DECT are always smaller than those of QCT. The BMD measurement correction equations in this study can render the measurements very close to the true values of the phantom, which further improves the accuracy of BMD measurements by DECT and QCT.

### Acknowledgments

The authors would like to acknowledge Joseph Elsom for his help in language refinement.

*Funding:* None.

### Footnote

*Reporting Checklist:* The authors have completed the MDAR reporting checklist. Available at <https://qims.amegroups.com/article/view/10.21037/qims-22-72/rc>

*Conflicts of Interest:* All authors have completed the ICMJE uniform disclosure form (available at <https://qims.amegroups.com/article/view/10.21037/qims-22-72/coif>). The authors have no conflicts of interest to declare.

*Ethical Statement:* The authors are accountable for all aspects of the work in ensuring that questions related to the accuracy or integrity of any part of the work are appropriately investigated and resolved. Our study was a phantom study which did not include a patient-based experiment or animal study, so ethical approval was not required.

*Open Access Statement:* This is an Open Access article distributed in accordance with the Creative Commons

Attribution-NonCommercial-NoDerivs 4.0 International License (CC BY-NC-ND 4.0), which permits the non-commercial replication and distribution of the article with the strict proviso that no changes or edits are made and the original work is properly cited (including links to both the formal publication through the relevant DOI and the license). See: <https://creativecommons.org/licenses/by-nc-nd/4.0/>.

### References

- Ioannidis G, Papaioannou A, Hopman WM, Akhtar-Danesh N, Anastassiades T, Pickard L, Kennedy CC, Prior JC, Olszynski WP, Davison KS, Goltzman D, Thabane L, Gafni A, Papadimitropoulos EA, Brown JP, Josse RG, Hanley DA, Adachi JD. Relation between fractures and mortality: results from the Canadian Multicentre Osteoporosis Study. *CMAJ* 2009;181:265-71.
- Sánchez-Riera L, Carnahan E, Vos T, Veerman L, Norman R, Lim SS, Hoy D, Smith E, Wilson N, Nolla JM, Chen JS, Macara M, Kamalaraj N, Li Y, Kok C, Santos-Hernández C, March L. The global burden attributable to low bone mineral density. *Ann Rheum Dis* 2014;73:1635-45.
- Cosman F, de Beur SJ, LeBoff MS, Lewiecki EM, Tanner B, Randall S, Lindsay R; National Osteoporosis Foundation. Clinician's Guide to Prevention and Treatment of Osteoporosis. *Osteoporos Int* 2014;25:2359-81.
- Link TM, Lang TF. Axial QCT: clinical applications and new developments. *J Clin Densitom* 2014;17:438-48.
- Engelke K, Mastmeyer A, Bousson V, Fuerst T, Laredo JD, Kalender WA. Reanalysis precision of 3D quantitative computed tomography (QCT) of the spine. *Bone* 2009;44:566-72.
- Engelke K. Quantitative Computed Tomography-Current Status and New Developments. *J Clin Densitom* 2017;20:309-21.
- Adams JE. Advances in bone imaging for osteoporosis. *Nat Rev Endocrinol* 2013;9:28-42.
- Bredella MA, Daley SM, Kalra MK, Brown JK, Miller KK, Torriani M. Marrow Adipose Tissue Quantification of the Lumbar Spine by Using Dual-Energy CT and Single-Voxel (1)H MR Spectroscopy: A Feasibility Study. *Radiology* 2015;277:230-5.
- Cheng X, Li K, Zhang Y, Wang L, Xu L, Liu Y, Duanmu Y, Chen D, Tian W, Blake GM. The accurate relationship between spine bone density and bone marrow in humans. *Bone* 2020;134:115312.
- Kuiper JW, van Kuijk C, Grashuis JL, Ederveen AG,

- Schütte HE. Accuracy and the influence of marrow fat on quantitative CT and dual-energy X-ray absorptiometry measurements of the femoral neck in vitro. *Osteoporos Int* 1996;6:25-30.
11. Bligh M, Bidaut L, White RA, Murphy WA Jr, Stevens DM, Cody DD. Helical multidetector row quantitative computed tomography (QCT) precision. *Acad Radiol* 2009;16:150-9.
  12. Yu EW, Thomas BJ, Brown JK, Finkelstein JS. Simulated increases in body fat and errors in bone mineral density measurements by DXA and QCT. *J Bone Miner Res* 2012;27:119-24.
  13. Aparisi Gómez MP, Ayuso Benavent C, Simoni P, Aparisi F, Guglielmi G, Bazzocchi A. Fat and bone: the multiperspective analysis of a close relationship. *Quant Imaging Med Surg* 2020;10:1614-35.
  14. Sanghavi PS, Jankharia BG. Applications of dual energy CT in clinical practice: A pictorial essay. *Indian J Radiol Imaging* 2019;29:289-98.
  15. Wichmann JL, Booz C, Wesarg S, Kafchitsas K, Bauer RW, Kerl JM, Lehnert T, Vogl TJ, Khan MF. Dual-energy CT-based phantomless in vivo three-dimensional bone mineral density assessment of the lumbar spine. *Radiology* 2014;271:778-84.
  16. Patino M, Prochowski A, Agrawal MD, Simeone FJ, Gupta R, Hahn PF, Sahani DV. Material Separation Using Dual-Energy CT: Current and Emerging Applications. *Radiographics* 2016;36:1087-105.
  17. Woisetschläger M, Hägg M, Spångeus A. Computed tomography-based opportunistic osteoporosis assessment: a comparison of two software applications for lumbar vertebral volumetric bone mineral density measurements. *Quant Imaging Med Surg* 2021;11:1333-42.
  18. Hales CM, Fryar CD, Carroll MD, Freedman DS, Ogden CL. Trends in Obesity and Severe Obesity Prevalence in US Youth and Adults by Sex and Age, 2007-2008 to 2015-2016. *JAMA* 2018;319:1723-5.
  19. Baum T, Cordes C, Dieckmeyer M, Ruschke S, Franz D, Hauner H, Kirschke JS, Karampinos DC. MR-based assessment of body fat distribution and characteristics. *Eur J Radiol* 2016;85:1512-8.
  20. Kalender WA, Felsenberg D, Genant HK, Fischer M, Dequeker J, Reeve J. The European Spine Phantom--a tool for standardization and quality control in spinal bone mineral measurements by DXA and QCT. *Eur J Radiol* 1995;20:83-92.
  21. Mu S, Wang J, Gong S. Application of Medical Imaging Based on Deep Learning in the Treatment of Lumbar Degenerative Diseases and Osteoporosis with Bone Cement Screws. *Comput Math Methods Med* 2021;2021:2638495.
  22. Engelke K, Adams JE, Armbrrecht G, Augat P, Bogado CE, Bouxsein ML, Felsenberg D, Ito M, Prevrhal S, Hans DB, Lewiecki EM. Clinical use of quantitative computed tomography and peripheral quantitative computed tomography in the management of osteoporosis in adults: the 2007 ISCD Official Positions. *J Clin Densitom* 2008;11:123-62.
  23. Cui X, Huang S, Han H, Yu W. Revolution CT Accuracy and repeatability of Revolution CT energy spectrum imaging in measurement of bone mineral density of spine phantom. *Chin J Interv Imaging Ther* 2020;17:430-3.
  24. Li X, Li X, Li J, Jiao X, Jia X, Zhang X, Fan G, Yang J, Guo J. The accuracy of bone mineral density measurement using dual-energy spectral CT and quantitative CT: a comparative phantom study. *Clin Radiol* 2020;75:320.e9-320.e15.
  25. Gao B, Zhang Y, Huang S, Cui X, Zhao Y, Yu W. Accuracy of low-dose quantitative CT for measuring lumbar bone mineral density in people with different body mass index. *Chin J Imaging Technol* 2021;37:1401-4.
  26. Javed F, Yu W, Thornton J, Colt E. Effect of fat on measurement of bone mineral density. *Int J Body Compos Res* 2009;7:37-40.
  27. Rodriguez-Granillo GA, Capunay C, Deviggiano A, De Zan M, Carrascosa P. Regional differences of fat depot attenuation using non-contrast, contrast-enhanced, and delayed-enhanced cardiac CT. *Acta Radiol* 2019;60:459-67.

**Cite this article as:** Ye H, Li X, Yao N, Shi Y, Wang Y, Yu W. Effect of abdominal adipose content on spine phantom bone mineral density measured by rapid kilovoltage-switching dual-energy CT and quantitative CT. *Quant Imaging Med Surg* 2022;12(10):4914-4923. doi: 10.21037/qims-22-72